Chemosphere 293 (2022) 133637

Contents lists available at ScienceDirect

Chemosphere

journal homepage: www.elsevier.com/locate/chemosphere

Characteristics of secondary organic aerosols tracers in $PM_{2.5}$ in three central cities of the Yangtze river delta, China

Chen Yang [a,b,c], Zhenyu Hong [a,b,c], Jinsheng Chen [a,b,*], Lingling Xu [a,b,**], Mazhan Zhuang [d], Zhi Huang [d]

[a] Center for Excellence in Regional Atmospheric Environment, Institute of Urban Environment, Chinese Academy of Sciences, Xiamen, 361021, China
[b] Key Lab of Urban Environment and Health, Institute of Urban Environment, Chinese Academy of Sciences, Xiamen, 361021, China
[c] University of Chinese Academy of Sciences, Beijing, 100049, China
[d] Xiamen Institute of Environmental Science, Xiamen, 361021, China

HIGHLIGHTS

- $PM_{2.5}$-bound SOA tracers in three central cities of the YRD region were investigated.
- Reasons for the differences of SOA tracers among sites and seasons were discussed.
- Implication of α/β-pinene SOA tracers for aerosol aging degree.
- Isoprene SOA tracers indicates the effects of large anthropogenic NO_2 emissions.

GRAPHICAL ABSTRACT

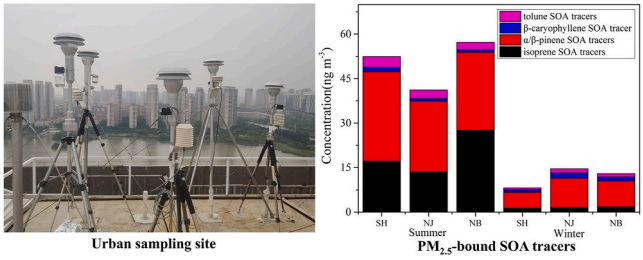

ARTICLE INFO

Handling Editor: Volker Matthias

Keywords:
Secondary organic aerosol
Organic tracers
The yangtze river delta region
Pollution characteristics
$PM_{2.5}$

ABSTRACT

Secondary organic aerosols (SOA) are important atmospheric pollutants that affect air quality, radiation, and human health. In this study, 14 typical SOA tracers were measured in $PM_{2.5}$ collected from three central cities of the Yangtze River Delta (YRD) region in the winter of 2014 and the summer of 2015. Among the determined SOA tracers, α/β-pinene SOA tracers contributed 55.9%, followed by isoprene SOA tracers (33.7%), anthropogenic benzene SOA tracer (6.4%) and β-caryophyllene SOA tracer (4.0%). There was no significant difference in the concentration of individual SOA tracers among the three cities ($p > 0.05$), indicating a high degree of regional consistency. The concentrations of isoprene, α/β-pinene, and toluene SOA tracers were significantly higher in summer than in winter. A correlation of SOA tracers with temperature implies that the isoprene and α/β-pinene SOA tracers in summer were greatly boosted by plant emissions and the high DHOPA in summer could be attributed to evaporation of paint and solvent. In contrast, the elevated β-caryophyllene SOA tracer in winter was likely associated with active biomass burning. Furthermore, we observed a close correlation of summer isoprene and α/β-pinene SOA tracers with sulfate only in Shanghai, which verifies that biogenic SOA formation was facilitated by high concentration of sulfate. The ratios of MGA/MTLs and P/M were applied to reveal the impact of NO_x on SOA formation and the aging degree of SOA, respectively. The MGA/MTLs ratios were comparable for

* Corresponding author. .Center for Excellence in Regional Atmospheric Environment, Institute of Urban Environment, Chinese Academy of Sciences, Xiamen, 361021, China.
** Corresponding author. Center for Excellence in Regional Atmospheric Environment, Institute of Urban Environment, Chinese Academy of Sciences, Xiamen, 361021, China.
E-mail addresses: jschen@iue.ac.cn (J. Chen), linglingxu@iue.ac.cn (L. Xu).

https://doi.org/10.1016/j.chemosphere.2022.133637
Received 6 August 2021; Received in revised form 22 December 2021; Accepted 13 January 2022
Available online 18 January 2022

the three cities, but much higher than the background value of this region as expected. The P/M ratios suggest that the aging degree of SOA in the YRD region was generally low, but the winter SOA were fresher than the summer SOA. Our research helps to understand pollution characteristics of SOA tracers in the urban agglomeration.

1. Introduction

Organic aerosols affect the distribution of precipitation through the formation of cloud condensation nuclei, thereby changing global climate conditions. At the same time, organic aerosols also affect atmospheric stability, and a slice of extinction components reduce atmospheric visibility (Nozière et al., 2015). Secondary organic aerosols (SOA) formed by the oxidation of organic gases account for the main part of atmospheric organic aerosols globally. Therefore, SOA have attracted considerable attention in recent years and have become a frontier and hot issue in the research of air pollution. Volatile organic compounds (VOCs) are very important in the formation of SOA (Ding et al., 2016). VOCs from anthropogenic emissions are mainly composed of alkanes, alkenes and aromatic hydrocarbons, the main sources of which include the burning of fossil fuels and the volatilization of organic solvents, while VOCs from natural sources are primarily comprised of isoprene, α/β-pinene and sesquiterpene compounds, etc. SOA generated from certain precursors result in unique tracers, which provides valuable insight into aerosol formation schemes (Kleindienst et al., 2007).

Identification of the relative abundance of different SOA tracers is important for pollution reduction. Isoprene oxidation products, i.e., MTLs (including 2-methylthreitol (MTL1) and 2-methylerythritol (MTL2)) in aerosols were first discovered in the Amazon forests (Claeys et al., 2004). After that, oxidation products of precursors VOCs, such as C5-alkene triols (Surratt et al., 2006), 2-methylglyceric acid (MGA) (Surratt et al., 2010), 2,3-dihydroxy-4-oxopentanoic acid (DHOPA) (Offenberg et al., 2007), 3-hydroxyglutaric acid (HGA) (Eddingsaas et al., 2012), β-caryophyllinic acid (Jaoui et al., 2007), have been successively identified in chamber experiments and field observations. Since existing analysis methods cannot identify all chemical components in SOA, the approach based on SOA tracer was widely used to analyze the characteristics and precursors of SOA (Alfarra et al., 2006; D'Ambro et al., 2017; Palm et al., 2017). A large-scale survey in China showed that SOA tracers were mainly derived from biological precursors, while the contribution of anthropogenic aromatics was very low (Ding et al., 2014). A large number of studies have proved that biological precursors are indeed the richest source of SOA tracers in China (Shen et al., 2015; Yuan et al., 2018; Hong et al., 2019). The concentrations of isoprene SOA tracers in the Pearl River Delta (PRD) region were much higher in summer than in winter, but the seasonal difference of α/β-pinene was minor (Ding et al., 2012). A study on forested area (Mt. Wuyi) in East China pointed out that concentrations of α/β-pinene and isoprene SOA tracers displayed a positive correlation with temperature, and a negative correlation with relative humidity (RH) (Ren et al., 2019). Recently, Ding et al. (2017) found that the concentration of anthropogenic 2,3-dihydroxy-4-oxopentanoic acid (DHOPA) tracer was significantly higher in cold seasons than in summer, which was linked to increased biomass combustion emissions. A field observation in urban area showed that the contribution of aromatic to total SOA tracers increased as pollution degree increased, which suggests that anthropogenic SOA precursors should be given serious consideration, especially during heavy pollution episodes (Liu et al., 2020).

The Yangtze River Delta (YRD) region is one of the three fastest-growing economic development regions in China. The YRD region has experienced severe haze pollution events in 2013, in which SOA contributed up to 35% of $PM_{2.5}$ and 71% of organic aerosols (Huang et al., 2014). Recent studies have shown that in the YRD urban areas, the concentration of SOA has maintained a high level during heavy $PM_{2.5}$ pollution episodes (Liu et al., 2020; Li et al., 2021). Thus, SOA plays an important role in haze pollution in the YRD region. The investigation concerning the characteristics of SOA in the YRD region were scarce. Existing research were mostly limited in one city of the YRD region, such as Nanjing (Liu et al., 2020; Li et al., 2020) and Shanghai (Feng et al., 2013; Zhu et al., 2018). In this study, we chose three central cities of the YRD region, i.e., Shanghai, Nanjing, and Ningbo to conduct field monitoring of SOA tracers in winter and summer. The purposes of this study are (1) to investigate the concentration levels, spatial and seasonal variations of SOA tracers in the YRD region; (2) to explore the influence of urban NO_x levels on SOA tracers; (3) to get a better understanding of the implication of SOA tracers for aerosol aging degree and contributing sources of SOA.

2. Materials and methods

2.1. Sampling sites

The observation of SOA tracers was conducted in Shanghai, Nanjing, and Ningbo, the YRD region. We set one sampling site in each city (Fig. S1). As a national central city, Shanghai is the most economically developed and densely populated city in China. Shanghai also has a huge industrial area and the world's largest port for cargo throughput. The sampling site in Shanghai (SH, 121° 25′ E, 31° 10′ N, 18.0 m a.g.l.) is located on the roof of a building in the Shanghai Institute of Environmental Sciences, Xuhui District, which is surrounded by a mixed commercial and residential area. Nanjing is the capital city of Jiangsu Province. The sampling site in Nanjing (NJ, 118° 46′ E, 32° 03′ N, 42.9 m a.g.l.) is located on the top of atmospheric science teaching building in the Drum Tower Campus of Nanjing University, which is surrounded by commercial and residential areas. Ningbo is located in Zhejiang Province and is the third largest port city in the world. Ningbo Petrochemical Economic and Technological Development Zone have a large number of petrochemical bases. Among them, Zhenhai Refinery is the nation's largest refining and chemical enterprise, which has an annual production of 25 million tons of oil and 1 million tons of ethylene ability. The sampling site in Ningbo (NB, 121° 33′ E, 29° 48′ N, 20.0 m a.g.l.) is located on the top floor of a teaching building of the University of Nottingham Ningbo, Yinzhou District, which is surrounded by some industrial factories.

2.2. Sample collection

The sampling campaigns were conducted in the winter of 2014 and the summer of 2015. 24 h $PM_{2.5}$ samples were collected continuously on preheated (500 °C, 4 h) quartz filters (8 × 10 in., Whatman) using a high-volume sampler (TH1000H, Wuhan Tianhong, China) at a flow rate of 1.05 m^3 min^{-1}. The average temperature and relative humidity (RH) of the three cities were 30.4 °C ~ 32.9 °C and 74.5% ~ 85.3% in summer and 6.6 °C ~ 12.0 °C and 61.4% ~ 69.5% in winter (Table S1). The sampling time was from 9 a.m. to 8 a.m. the next day and the effective duration of each sample was guaranteed to exceed 20 h. Filter samples that did not meet the sampling time requirement were invalidated. In this study, 22 p.m.$_{2.5}$ filter samples were collected from each city. The sampled filters were covered with aluminum foil and stored at −20 °C until analysis.

2.3. Chemical analysis

Aliquots of quartz filter (ca. 2.5 cm^2) were cut, added with 10 mL of

dichloromethane/me-thanol (2:1, v/v), and performed ultrasonic extraction 3 times for 10 min. The extract was filtered into a pear-shaped bottle through a Pasteur pipette filled with quartz cotton and concentrated to less than 1 mL by a rotary evaporator (RE52-AA, Shanghai Yarong). The concentrated solution was transferred to a 1.5 mL chromatography flask. Meanwhile, rinsed the pear-shaped flask with an appropriate amount of solvent, and then merged into the chromatography flask. After that, the chromatographic bottle was dried on a nitrogen purifier, added with 60 μL of N, O-bis-(trimethylsilyl) trifluoroacetamide/pyridine (5:1, v/v), and derivatized in an oven at 70 °C for 3 h. After reaction, the solution was cooled, and added with 140 μL of tridecane (1.512 ng μL^{-1}) as an internal standard. The measurement was performed by a gas chromatography mass spectrometer (GC-MS, Agilent 7890A/5975C, US). GC-MS parameters were set as follows: kept initial temperature at 60 °C for 10 min, raised it to 300 °C at a rate of 5 °C min^{-1} and kept it for 40 min, and set the ion source temperature to 290 °C.

Levoglucosan, malic acid, 3-hydroxyglutaric acid (HGA), pinonic acid (PNA) and pinic acid (PA) were quantified using authentic standards. Because of the lack of commercial standards, α/β-pinene SOA tracers including 3-methyl-1, 2, 3-butanetricarboxylic acid (MBTCA), 3-acetyl glutaric acid (AGA), and 3-hydro-4,4-dimethyglutaric acid (HDMGA) were determined using malic acid as a standard. β-Caryophyllinic acid was estimated using the response factor of PA. Isoprene SOA tracers including 2-methylglyceric acid (MGA), C5-alkene triols (*cis*-2-methyl-1,3,4-trihydroxy-1-butene, *trans*-2-methyl-1,3,4-trihydroxy-1-butene, and 3-methyl-2,3,4-trihydroxy-1-butene), and 2-methyltetrols (MTLs) were quantified using erythritol as a standard (Fu et al., 2010; El Haddad et al., 2011).

2.4. Quality control and quality assurance

Field blanks were collected during the sampling periods by using filters on the sampler without pumping any air for 24 h. After being extracted and measured in the same way as the field samples, none of the targeted compounds were measured in the field blanks. The recovery rates of erythritol, HGA, PNA, PA, and malic acid were 71 ± 6%, 85 ± 10%, 62 ± 11%, 65 ± 7%, and 85 ± 8%, respectively. For duplicate samples (n = 5), the concentration of target compounds all differed by less than 13%. The reported concentrations of SOA tracers were not corrected for the recovery.

2.5. Data analysis

Relationships among different SOA tracers were investigated by Pearson correlation analysis. Seasonal and spatial differences in concentration and proportion of SOA tracers were examined by one-way ANOVA (Analysis of Variance).

3. Results and discussion

3.1. Concentrations and seasonal trends of SOA tracers

The average concentrations of total SOA tracers in SH, NJ, and NB were 30.32 ± 46.25, 27.90 ± 45.44, and 35.07 ± 22.68 ng m^{-3}, respectively (Table 1). As can be seen from Fig. 1, there were similar seasonal changes in the three cities: the concentrations of SOA tracers were significantly higher in summer than in winter ($p < 0.01$). Among all the SOA tracers, α/β-pinene SOA tracers contributed 55.9%, followed by isoprene SOA tracers (33.7%), anthropogenic benzene SOA tracer (6.4%), and β-caryophyllene SOA tracer (4.0%).

3.1.1. Isoprene SOA tracers

Two MTLs, MGA and three C5-alkene triols were determined as isoprene tracers. The concentrations of isoprene SOA tracers in SH, NJ and NB were 17.17, 13.50 and 27.54 ng m^{-3} in summer and 1.30, 1.55 and 1.80 ng m^{-3} in winter, respectively. There was no significant difference in the concentration of isoprene SOA tracers among the three sites ($p > 0.05$). Table 2 summarizes concentrations of SOA tracers in different regions of the world in previous studies. We found that the concentrations of isoprene SOA tracers varied considerably from one site to another. The summer concentrations of isoprene SOA tracers in the YRD region were in the same order of magnitude as those of Chinese megacities such as Guangzhou (27.89 ng m^{-3}, Yuan et al., 2018) and Shanghai (7.36 ng m^{-3} in May 22-June 19, Zhu et al., 2018). Mt. Wuyi is located in a complete ecological diversity forest. Since there were no anthropogenic point sources, it was considered as the regional background of the YRD region (Hong et al., 2019). The isoprene SOA tracers in Mt. Wuyi was obviously higher than those in the YRD cities, which was likely due to its lush vegetation. Previous Study has proved that isoprene is a major biogenic volatile organic compound (VOC) emitted

Table 1
Concentrations of secondary organic aerosol (SOA) tracers during the study period in SH, NJ and NB.

Species	SOA tracer concentration (ng m^{-3})		
	SH	NJ	NB
Isoprene SOA tracer			
MGA	0.84	0.92	0.85
MTL	5.77	5.32	11.57
MTL1	*1.79*	*1.49*	*3.08*
MTL2	*3.98*	*3.83*	*8.48*
C5-alkene triols	2.63	1.28	2.25
cis-2-methyl-1,3,4-trihydroxy-1-butene	*0.68*	*0.27*	*0.61*
3-methyl-2,3,4-trihydroxy-1-butene	*0.33*	*0.19*	*0.40*
trans-2-methyl-1,3,4-trihydroxy-1-butene	*1.62*	*0.81*	*1.25*
Sum of isoprene SOA tracer	9.24	7.52	14.67
α/β-pinene SOA tracer			
HGA	9.54	9.27	8.67
PA	1.05	1.14	1.42
PNA	2.10	2.14	1.78
MBTCA	1.01	1.15	2.19
AGA	0.34	0.37	0.60
HDMGA	3.70	2.80	0.86
Sum of α/β-pinene SOA tracer	17.74	16.87	17.52
Toluene SOA tracer			
DHOPA	2.06	2.11	1.78
β-caryophyllene SOA tracer			
β-caryophyllinic acid	1.28	1.40	1.14
Total SOA tracers	30.32	27.90	35.07

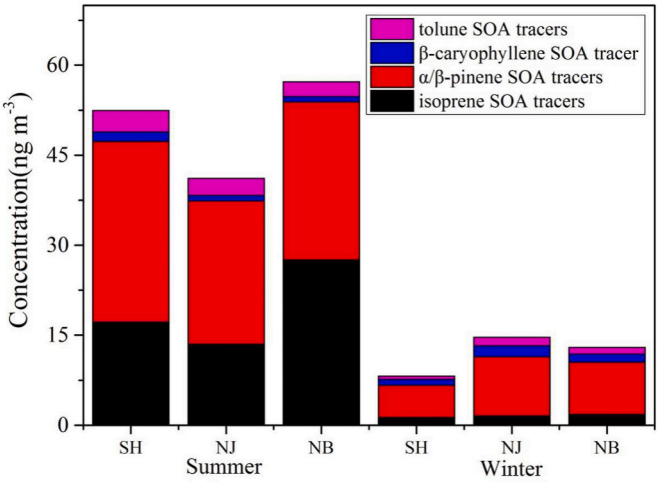

Fig. 1. Seasonal variations of $PM_{2.5}$-bound SOA tracers in SH, NJ and NB.

Table 2
Concentrations (ng m^{-3}) of SOA tracers in SH, NJ and NB and in other regions of the world.

Sampling site	Sampling type	Sampling period	Isoprene products	α/β-pinene products	β-caryophyllene products	Aromatics products	Reference
SH	$PM_{2.5}$	Summer	17.17	30.12	1.60	3.57	This study
SH	$PM_{2.5}$	Winter	1.30	5.36	0.96	0.54	This study
NJ	$PM_{2.5}$	Summer	13.50	23.88	0.94	2.85	This study
NJ	$PM_{2.5}$	Winter	1.55	9.86	1.86	1.37	This study
NB	$PM_{2.5}$	Summer	27.54	26.33	0.93	2.44	This study
NB	$PM_{2.5}$	Winter	1.80	8.71	1.35	1.09	This study
Hong Kong, China	$PM_{2.5}$	Summer	30	198	13	NA	Hu et al. (2008)
14 sites, China	$PM_{2.5}$	Summer	123	10.5	5.07	2.9	Ding et al. (2014)
Mexico City	$PM_{2.5}$	Spring	32.8	51.8	0.2	12.3	Stone et al. (2010)
Tibetan Plateau	Size-segregated particle	Four seasons	26.6	0.97	0.09	0.25	Shen et al. (2015)
Mumbai, India	PM_{10}	Winter	1.1	29	NA	0.62	Fu et al. (2016)
Mt. Tai Mo Shan	$PM_{2.5}$	Fall	54.7	26.3	1.1	2.1	Lyu et al. (2017)
Himalayas	$PM_{2.5}$	Summer	30.7	13.2	1.6	NA	Stone et al. (2012)
Alert, Canada	$PM_{2.5}$	Winter-Summer	0.3	1.6	0.12	NA	Fu et al. (2009)
Shanghai, China	$PM_{2.5}$	Summer-Spring	7.36	2.76	0.58	NA	Zhu et al. (2018)
Guangzhou, China	$PM_{2.5}$	Four seasons	27.89	28.21	9.25	NA	Yuan et al. (2018)
The PRD region, China	$PM_{2.5}$	Summer	126	11.6	2.87	17.8	Ding et al. (2012)
The PRD region, China	$PM_{2.5}$	Fall-Winter	25.1	16.4	3.25	13.1	Ding et al. (2012)
Mt. Wuyi, China	$PM_{2.5}$	Four seasons	45.28	30.66	5.99	0.62	Hong et al. (2019)

"NA" means not available.

by the biosphere into the atmosphere (Cappellin et al., 2019). High concentrations of isoprene SOA tracers in summer were probably associated with high air temperature, rapid growth of plants, sufficient light and high humidity (Ding et al., 2012; Yuan et al., 2018). In this study, the concentrations of isoprene SOA tracers were an order of magnitude higher in summer than in winter ($p < 0.001$). The proportion of isoprene SOA tracers in total SOA tracers was 38.6% in summer versus 13.0% in winter. We have observed significant correlations of isoprene SOA tracers with temperature ($R^2 = 0.27$ in summer and 0.35 in winter, $p < 0.05$, Fig. S2), indicating that the promotion of isoprene SOA tracer formation by temperature. It is worth noting that the slope of isoprene SOA tracers vs. temperature was remarkably higher in summer (slope = 4.02) than in winter (slope = 0.14). The steeper slope in summer implied a stronger promotion of isoprene emissions, which is consistent with a previous result that the plant emission rate of isoprene depended on temperature (Ding et al., 2016). Therefore, the enhanced plant emissions in summer due to high temperature (Table S1) could largely explain the seasonal pattern of isoprene SOA tracers.

Additionally, we have found a strong correlation of isoprene SOA tracers, as well as α/β-pinene SOA tracers with sulfate in summer ($R^2 = 0.83$ and 0.85, respectively, $p < 0.05$, Fig. S4a, b), which occurred in Shanghai but not in other two cities. It was reported that the correlation between biogenic SOA tracers and sulfate varied across cities and seasons. Moreover, the strong correlation between biogenic SOA and sulfate was observed in sulfate-rich plums (Xu et al., 2015) and the areas of high anthropogenic pollution such as the southeastern United States and the North China Plain of China (Rattanavaraha et al., 2017; Li et al., 2018). A recent real-time observation in North China Plain (Gucheng) revealed a facilitation of isoprene SOA formation caused by the increase of sulfate (Li et al., 2018). Their study reported that, on the one hand, sulfate provides a surface favorable for acid-catalyzed reaction uptake and ring opening of key intermediates in the gas phase, and on the other hand the salting effect of sulfate increases the solubility of isoprene SOA tracers. In this study, the close correlation between biogenic tracers and sulfate in Shanghai was likely associated with the relatively high concentrations of sulfur dioxide and sulfate in this city (Table S1).

3.1.2. *α/β-pinene SOA tracers*

Six organic acids, i.e., HGA, PNA, PA, AGA, HDMGA, and MBTCA, were identified as α/β-pinene oxidation products in this study. The concentrations of α/β-pinene SOA tracers for SH, NJ, and NB were 30.12, 23.88, and 26.33 ng m^{-3} in summer and 5.36, 9.86, and 8.71 ng m^{-3} in winter, respectively. No significant difference was observed in the concentrations of α/β-pinene SOA tracers among the three cities either in winter or in summer ($p > 0.05$). The average concentration of α/β-pinene SOA tracers in the YRD cities was approximately half of that in Mt. Wuyi (Table 2). That is mainly because the vegetation is dense in Mt. Wuyi and natural sources are the main contributors of α/β-pinene. The seasonal trend with higher α/β-pinene SOA tracers in summer than in winter in the YRD region ($p < 0.001$) is consistent with those in the southeastern and Midwestern United States (Kleindienst et al., 2007; Lewandowski et al., 2008). Similar to isoprene SOA tracers, α/β-pinene SOA tracers showed significant correlations with temperature and a deeper slope in summer (slope = 3.36) than in winter (slope = 0.92) (Fig. S3b), which indicated a strong promotion of α/β-pinene emissions in summer. In addition, we found a significant correlation between α/β-pinene SOA tracers and ozone in summer (Fig. S3a). The oxidation by OH radicals was thought to be the dominant process of the removal of biogenic VOCs in the atmosphere (Kleindienst et al., 2007). However, recent studies have demonstrated that α-pinene can react with ozone to form stabilized Criegee intermediates (sCI), which are subsequently oxidized and eventually partition to the aerosol phase to form SOA (Kristensen et al., 2014). In this study, the correlation of ozone with α/β-pinene in summer suggests that, in addition to OH-initiated oxidation, α/β-pinene ozonolysis was also a potential pathway for α/β-pinene SOA formation.

3.1.3. *β-caryophyllene SOA tracer*

β-caryophyllene is one of the most abundant sesquiterpenes, and the most typical tracer is β-caryophyllinic acid (Jaoui et al., 2007). The

concentrations of β-caryophyllene SOA tracer in SH, NJ and NB were 1.60, 0.94 and 0.93 ng m^{-3} in summer and 0.96, 1.86 and 1.35 ng m^{-3} in winter (Table 1), respectively, which accounted for less than 5% of total SOA tracers. The concentrations of β-caryophyllene SOA tracer in our study were comparable with the results of a study conducted in Shanghai (0.58 ng m^{-3} in May 22-June 19, Zhu et al., 2018). Distinguished from isoprene SOA tracers and α/β-pinene SOA tracers, β-caryophyllene SOA tracer was the only detected tracer without significant seasonal difference ($p > 0.05$). Thus, plant emissions were unlikely the major contribution of β-caryophyllene SOA tracer in the YRD region.

3.1.4. Toluene SOA tracer

As the SOA tracer of anthropogenic benzene compounds, the concentrations of DHOPA for SH, NJ, and NB were 3.57, 2.85, and 2.44 ng m^{-3} in summer and 0.54, 1.37, and 0.39 ng m^{-3} in winter, respectively (Table 1). The concentrations of DHOPA showed no significant spatial difference ($p > 0.05$) and they were all higher in summer than in winter ($p < 0.001$). The concentrations of DHOPA in the YRD region were higher than those in Mt. Wuyi (0.62 ng m^{-3} in four seasons, Hong et al., 2019) and the background site in China (Tibetan plateau, 0.25 ng m^{-3} in four seasons, Shen et al., 2015), but much lower than that in the PRD region (17.8 ng m^{-3} in summer, 13.1 ng m^{-3} in fall-winter, Ding et al., 2012). Previous studies have revealed that the levels of aromatics in the PRD region were almost the highest as compared to other regions of China due to large emissions from vehicular exhaust and leakage of liquefied petroleum gas into the atmosphere (Tang et al., 2008).

3.2. Isoprene SOA tracers relating to NO_x level

The percentages of MGA, C5-alkene triols, MTL1 and MTL2 in total isoprene SOA tracers in different seasons are shown in Fig. 2. MTLs accounted for the highest proportion of isoprene SOA tracers with a value of 62.4%~78.9%, followed by C5-alkanes triols (14.3%~28.5%) and MGA (5.8%~12.2%). There was no significant difference in the proportion of MGA among the three cities ($p > 0.05$). However, the seasonal difference of MGA was the greatest among the four isoprene SOA tracers, with a proportion of 34.8% in winter and 6.8% in summer. It can be seen that the percentages of MGA were considerably higher in winter (34.8%) than in summer (6.8%). On the basis of chamber simulation (Zhang et al., 2011) and ambient observation (Zhu et al., 2018), unlike other isoprene SOA tracers, the formation of MGA was suggested to be favored by low RH. Thus, the reason for the seasonal variation of MGA proportion may be that MGA was formed more easily in winter with lower RH (65.4%) than in summer with higher RH (79.9%).

There are two main pathways for the oxidation of isoprene in the atmosphere: a) Under low NO_x conditions, oxidation of isoprene by OH and HO_2 radicals to produce isoprene epoxydiols (IEPOX), which can generate C5-alkene triols and MTLs by reactive uptake. b) Under high NO_x conditions, methacrylic acid epoxide (MAE) and hydroxymethyl-methyl-lactone (HMML) are the products of isoprene undergoing multiple oxidation reactions with RO_2, NO_x and OH radicals, which eventually undergo further reactions to produce MGA (Surratt et al., 2010; Lin et al., 2013). Therefore, the ratio of MGA/MTLs has been used to reveal the impact of NO_x on SOA formation in extensive research (Paulot et al., 2009; Surratt et al., 2010; Ding et al., 2012; Hong et al., 2019). The ratios of MGA/MTLs in SH, NJ, and NB were 0.13, 0.16, and 0.16 in summer, while in winter they were 0.63, 0.72, and 0.88, respectively (Fig. 3b). The MGA/MTLs ratios did not show spatial differences ($p > 0.05$), neither did NO_2 concentration ($p > 0.05$). In addition, the ratios of MGA/MTLs were significantly higher in winter than in summer, which is consistent with the change of NO_2 concentration (33.3 ± 10.07 μg m^{-3} in summer, 64.4 ± 25.67 μg m^{-3} in winter). The MGA/MTLs ratios in this study are close to those reported in Shanghai, where the ratios were 0.10 in summer and 0.91 in winter (Feng et al., 2013), but much higher than those in the Mt. Wuyi (0.01 in summer, 0.22 in fall-winter, Hong et al., 2019), suggesting that the YRD region was affected more by NO_2 emission sources.

Although both MTLs and C5-alkanes triols are important isoprene SOA tracers in the conditions of low-NO_x, their formation mechanisms are slightly different (Shrivastava et al., 2017). MTLs and C5-alkanes triols maintained good correlations in all cities, both in summer and winter, indicating that their main sources were consistent in the YRD region. However, we noted that the slope of MTLs vs. C5-alkanes triols was much steeper in NB-summer (slope = 5.29) than in others city-season (Fig. S6). Recent work has shown that the yield of C5-alkanes triols decreases and the slope becomes steeper as the pH of the particle increases (Yee et al., 2020). Due to the lack of data on the pH of particles in this study, we referred to other studies in the similar periods and found that the concentration of hydrogen ions in $PM_{2.5}$ in Ningbo was lower than in Nanjing and Shanghai (68.22 nmol m^{-3} in SH, Ming et al., 2017; 183.44 nmol m^{-3} in NB, Zhang et al., 2019; 7.97 nmol m^{-3} in NB, Xu et al., 2017). This implies that the steeper slope of MTLs vs. C5-alkanes triols in Ningbo in summer was likely associated with the pH of particles.

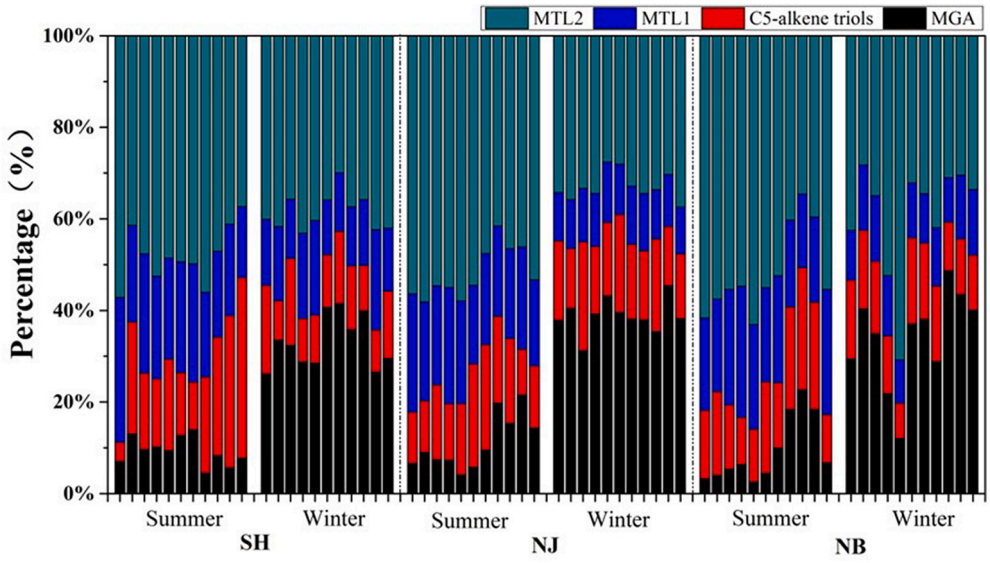

Fig. 2. Percentages of $PM_{2.5}$-bound isoprene SOA tracers in SH, NJ and NB.

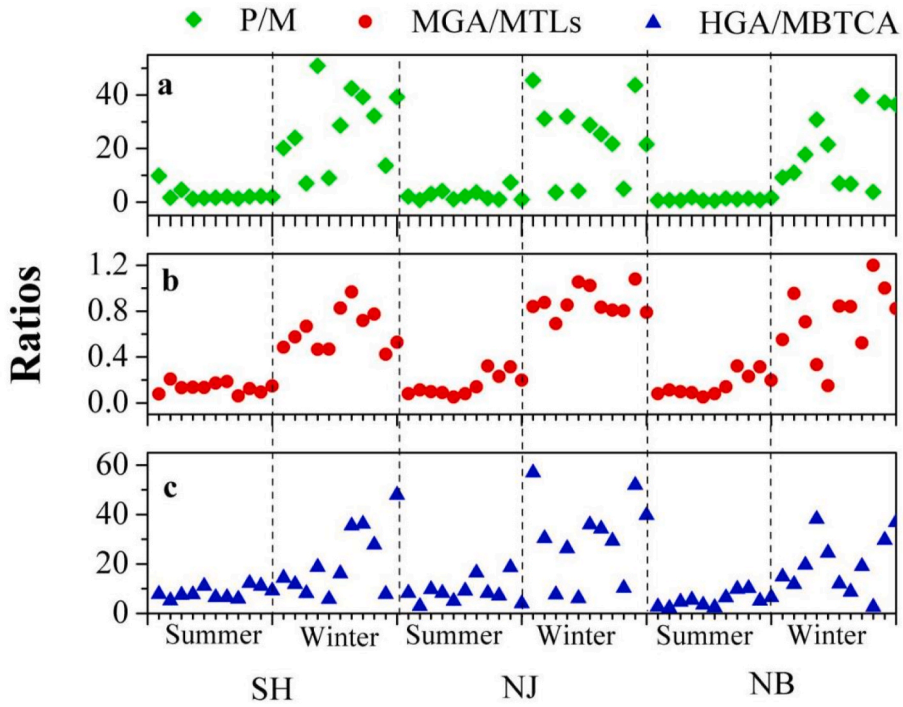

Fig. 3. Concentration ratios of $PM_{2.5}$-bound SOA tracers in SH, NJ and NB.

3.3. α/β-pinene SOA tracer relating to aerosol aging

The percentages of MBTCA, HDMGA, AGA, HGA, PNA and PA in total α/β-pinene SOA tracers in different seasons are shown in Fig. 4. PA, PNA in the ambient aerosols are produced by photooxidation of α/β-pinene via reactions with O_3 and OH radicals, which are generally considered to be the first-generation products of α/β-pinene (Szmigielski et al., 2007). The formation of MBTCA can be explained by further reaction of *cis*-pinonic acid with OH radical (Eddingsaas et al., 2012), thus it has been considered as a higher-generation product. A high P/M ratio demonstrates less transformation of PNA and PA to MBTCA and thus indicates relatively fresh α/β-pinene SOA, and vice versa (Ding et al., 2014). The average P/M ratios in SH, NJ and NB were 2.74, 2.54 and 1.06 in summer and 27.89, 23.89 and 20.14 in winter (Fig. 3a), respectively. We did not observe a significant difference in P/M ratio among the three cities ($p > 0.05$), indicating that the aging degree of SOA in the YRD region was similar. Chamber research demonstrated that the P/M ratios in newly formed α/β-pinene SOA ranged from 1.51 to 3.21 (Offenberg et al., 2007). The winter P/M ratios of this study are remarkably higher than those in newly formed α/β-pinene SOA, and also higher than those reported from the YRD region (0.48 in summer, 2.17 in fall-winter, Ding et al., 2012). The results suggest that the winter α/β-pinene SOA tracers in the YRD was relatively fresh. By comparison, the low P/M ratio in summer suggested that there were more secondary transformations in summer in the YRD regions. A previous study has proved that strong solar radiation in summer favored the formation of MBTCA (Feng et al., 2013). On the other hand, PNA, the most volatile among α/β-pinene SOA tracers, will be more partitioned in particle

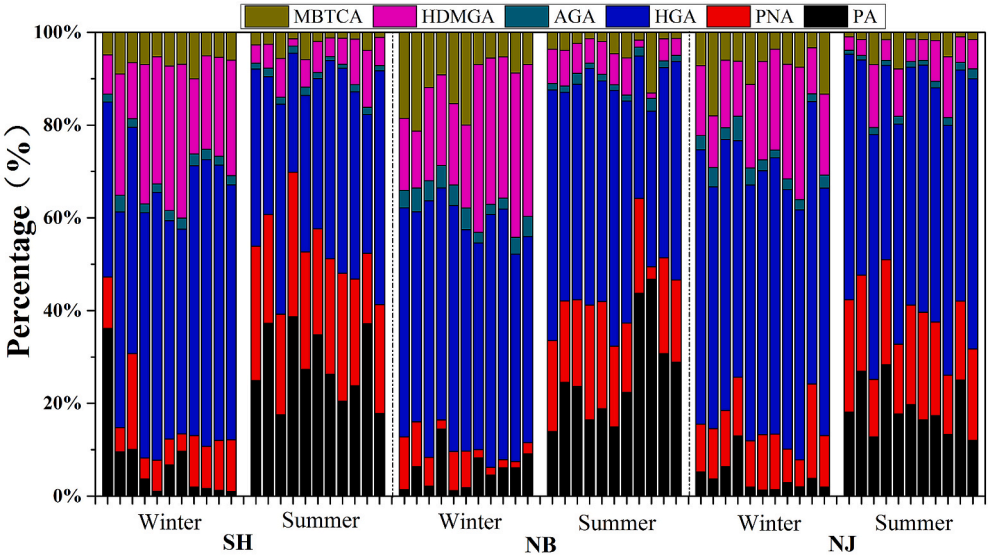

Fig. 4. Percentages of $PM_{2.5}$-bound α/β-pinene SOA tracers in SH, NB and NJ.

phase under low temperature conditions in winter. Therefore, the seasonal pattern of higher P/M ratios in winter than in summer could be attributed to the effects of gas-particle partition and photochemical reactions.

Both HGA and MBTCA are more aged products formed by further reaction of α/β-pinene. Several previous studies suggested that HGA/MBTCA ratio can be used to distinguish different α/β-pinene, among which α-pinene has a higher yield of MBTCA, while β-pinene generates more HGA (Jaoui et al., 2005; Ding et al., 2014). In this study, the ratio of HGA/MBTCA did not exhibit significant differences among the three cities ($p > 0.05$). The ratio ranged from 5.35 to 8.88 in summer (Fig. 3c), which is higher than those in 14 sites in China (0.75–5.07 in summer, Ding et al., 2014) and Mt. Wuyi (1.77 in summer, Ding et al., 2014). The results suggest that β-pinene made a greater contribution to α/β-pinene SOA in the YRD region. In terms of seasonal distribution, HGA/MBTCA ratios in winter were significantly higher than those in summer ($p < 0.05$), indicating that the contribution of β-pinene to α/β-pinene SOA increased in winter when natural sources substantially reduced.

3.4. SOA tracers relating to anthropogenic sources

3.4.1. β-caryophyllene SOA tracer

Sesquiterpene (such as β-caryophyllene) could accumulate in wood and leaves due to its lower volatility, and then emitted in large amounts during biomass burning (Ciccioli et al., 2014). Existing research has specified that levoglucosan is an excellent tracer of biomass combustion (Simoneit et al., 2002). In order to study the effect of biomass combustion on β-caryophyllene SOA tracer, the correlation analysis between levoglucosan and β-caryophyllic acid was performed. As showed in Fig. 5, the correlations between levoglucosan and β-caryophyllic acid in winter were relatively close, with the R^2 of 0.79, 0.73 and 0.65 in SH, NJ, and NB, respectively. The good correlations manifest that the sources of levoglucosan and β-caryophyllic acid might be consistent and biomass burning was likely the main source of β-caryophyllic acid in winter. However, in summer, the correlations between levoglucosan and β-caryophyllic acid in the three cities were quite different ($R^2 = 0.78$ in SH; $R^2 = 0.15$ in NJ; $R^2 = 0.93$ in NB). The concentration of levoglucosan in summer was only one-seventh of that in winter, which suggests that biomass burning was probably not the dominant source for β-caryophyllic acid in summer. These results were supported by the fewer field biomass burning events in summer than in winter (Fig. S6). Other factors, like plant emissions (Zhu et al., 2018), might also make an important contribution to β-caryophyllene SOA in the warm season, which affects the correlations between levoglucosan and β-caryophyllic acid in summer.

3.4.2. Benzene series SOA tracer

The concentrations of DHOPA in the YRD region were significantly higher in summer than in winter ($p < 0.001$), which is contrary to those at 12 sites in China (1.61 ng m^{-3} in summer, 4.78 ng m^{-3} in winter, Ding et al., 2017). Extensive researches have revealed that benzene series in China mainly come from power plants, industrial processes, motor vehicle emissions, solvent use, oil volatilization, coal combustion and biomass combustion (Ding et al., 2017). However, an Asian emission source inventory pointed out that the aromatic hydrocarbons produced by power plants, industrial processes and transportation almost have no seasonal changes (Zhang et al., 2009). In this study, DHOPA was found to correlate well with levoglucosan (Fig. S7c), but the more active biomass burning in winter than in summer could not explain the seasonal variation of DHOPA. On the other hand, there was a positive correlation between temperature and DHOPA (Fig. S7b), and the slope of DHOPA vs. temperature was about three times higher in summer than in winter. Toluene is the precursor of DHOPA, and C7–C9 aromatics are major constituents of VOCs emitted from paints and solvents use (Zhang et al., 2013; Mo et al., 2015). Thus, the high temperature in summer would promote the evaporation of paint and solvent to release more

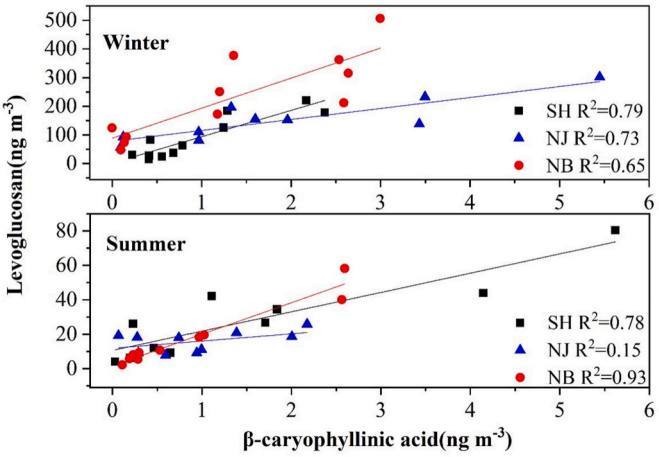

Fig. 5. Correlation between levoglucosan and β-caryophyllinic acid.

precursors of DHOPA. In addition, we found a significant correlation between DHOPA and ozone in summer (Fig. S7a), suggesting the more formation of DHOPA under the high oxidized condition.

4. Conclusions

This paper determined 14 typical $PM_{2.5}$-bound SOA tracers in three cities of the YRD region in the winter of 2014 and the summer of 2015. Biogenetic SOA tracers, i.e., isoprene and α/β-pinene SOA tracers contributed nearly 90% of the total determined SOA tracers. There was no significant difference in the concentration of individual SOA tracers among the three cities ($p > 0.05$), indicating a high degree of regional consistency. The higher levels of biogenetic SOA tracers in summer than in winter were mainly due to the emissions of plant emissions, while the increase of DHOPA in summer could be attributed to elevated evaporation of paint and solvent. In contrast, the elevated β-caryophyllene SOA tracer in winter was likely associated with active biomass burning. Furthermore, we found that biogenic SOA formation was facilitated by high concentration of sulfate in Shanghai. In the YRD region, the ozonolysis of precursors could also be a potential way for α/β-pinene SOA tracers and DHOPA formation in summer. The MGA/MTLs ratios in the YRD region were much higher than the background value of this region, indicating a large amount of anthropogenic NO_2 emissions in the YRD region. The P/M ratios suggest that the aging degree of SOA in the YRD region was generally low, especially in winter, as compared to the PRD region in China.

Credit author statement

Chen Yang: Data curation, Writing – original draft, Writing – review & editing, Visualization; **Zhenyu Hong:** Validation, Writing – review & editing; **Jinsheng Chen:** Resources, Project administration, Writing – review & editing, Supervision; **Lingling Xu:** Conceptualization, Writing – review & editing, Supervision; **Mazhan Zhuang:** Investigation, Methodology; **Zhi Huang:** Conceptualization, Validation.

Declaration of competing interest

The authors declare that they have no known competing financial interests or personal relationships that could have appeared to influence the work reported in this paper.

Acknowledgement

This study was funded by the Cultivating Project of Strategic Priority Research Program of Chinese Academy of Sciences (XDPB1903), the

National Key Research and Development Program (2016YFC02005, 2016YFC0112200), the National Natural Science Foundation of China (U1405235), the Center for Excellence in Regional Atmospheric Environment, CAS (E0L1B20201), the Xiamen Youth Innovation Fund Project (3502Z20206094), State Key Laboratory of Environmental Chemistry and Ecotoxicology, Research Center for Eco-Environmental Sciences, CAS (KF2020-06), and Xiamen Atmospheric Environment Observation and Research Station of Fujian Province.

Appendix A. Supplementary data

Supplementary data to this article can be found online at https://doi.org/10.1016/j.chemosphere.2022.133637.

References

Alfarra, M.R., Paulsen, D., Gysel, M., Garforth, A.A., Dommen, J., Prévôt, A.S.H., Worsnop, D.R., Baltensperger, U., Coe, H., 2006. A mass spectrometric study of secondary organic aerosols formed from the photooxidation of anthropogenic and biogenic precursors in a reaction chamber. Atmos. Chem. Phys. 6, 5279–5293. https://doi.org/10.5194/acp-6-5279-2006.

Cappellin, L., Loreto, F., Biasioli, F., Pastore, P., McKinney, K., 2019. A mechanism for biogenic production and emission of MEK from MVK decoupled from isoprene biosynthesis. Atmos. Chem. Phys. 19, 3125–3135. https://doi.org/10.5194/acp-19-3125-2019.

Ciccioli, P., Centritto, M., Loreto, F., 2014. Biogenic volatile organic compound emissions from vegetation fires. Plant Cell Environ. 37, 1810–1825. https://doi.org/10.1111/pce.12336.

Claeys, M., Graham, B., Vas, G., Wang, W., Vermeylen, R., Pashynska, V., Cafmeyer, J., Guyon, P., Andreae, M.O., Artaxo, P., Maenhaut, W., 2004. formation of secondary organic aerosols through photooxidation of isoprene. Science 303, 1173–1176. https://doi.org/10.1126/science.1092805.

D'Ambro, E.L., Lee, B.H., Liu, J., Shilling, J.E., Gaston, C.J., Lopez-Hilfiker, F.D., Schobesberger, S., Zaveri, R.A., Mohr, C., Lutz, A., Zhang, Z., Gold, A., Surratt, J.D., Rivera-Rios, J.C., Keutsch, F.N., Thornton, J.A., 2017. Molecular composition and volatility of isoprene photochemical oxidation secondary organic aerosol under low- and high-NOx conditions. Atmos. Chem. Phys. 17, 159–174. https://doi.org/10.5194/acp-17-159-2017.

Ding, X., He, Q.-F., Shen, R.-Q., Yu, Q.-Q., Wang, X.-M., 2014. Spatial distributions of secondary organic aerosols from isoprene, monoterpenes, β-caryophyllene, and aromatics over China during summer. J. Geophys. Res. Atmos. 119 (11) https://doi.org/10.1002/2014jd021748, 877-811,891.

Ding, X., He, Q.-F., Shen, R.-Q., Yu, Q.-Q., Zhang, Y.-Q., Xin, J.-Y., Wen, T.-X., Wang, X.-M., 2016. Spatial and seasonal variations of isoprene secondary organic aerosol in China: significant impact of biomass burning during winter. Sci. Rep. 6 https://doi.org/10.1038/srep20411, 20411-20411.

Ding, X., Wang, X.-M., Gao, B., Fu, X.-X., He, Q.-F., Zhao, X.-Y., Yu, J.-Z., Zheng, M., 2012. Tracer-based estimation of secondary organic carbon in the Pearl River Delta, south China. J. Geophys. Res. Atmos. 117 https://doi.org/10.1029/2011jd016596 n/a-n/a.

Ding, X., Zhang, Y.-Q., He, Q.-F., Yu, Q.-Q., Wang, J.-Q., Shen, R.-Q., Song, W., Wang, Y.-S., Wang, X.-M., 2017. Significant increase of aromatics-derived secondary organic aerosol during fall to winter in China. Environ. Sci. Technol. 51, 7432–7441. https://doi.org/10.1021/acs.est.6b06408.

Eddingsaas, N.C., Loza, C.L., Yee, L.D., Seinfeld, J.H., Wennberg, P.O., 2012. α-pinene photooxidation under controlled chemical conditions – Part 1: gas-phase composition in low- and high-NOx; environments. Atmos. Chem. Phys. 12, 6489–6504. https://doi.org/10.5194/acp-12-6489-2012.

El Haddad, I., Marchand, N., Temime-Roussel, B., Wortham, H., Piot, C., Besombes, J.L., Baduel, C., Voisin, D., Armengaud, A., Jaffrezo, J.L., 2011. Insights into the secondary fraction of the organic aerosol in a Mediterranean urban area: Marseille. Atmos. Chem. Phys. 11, 2059–2079. https://doi.org/10.5194/acp-11-2059-2011.

Feng, J., Li, M., Zhang, P., Gong, S., Zhong, M., Wu, M., Zheng, M., Chen, C., Wang, H., Lou, S., 2013. Investigation of the sources and seasonal variations of secondary organic aerosols in PM2.5 in Shanghai with organic tracers. Atmos. Environ. 79, 614–622. https://doi.org/10.1016/j.atmosenv.2013.07.022.

Fu, P., Aggarwal, S.G., Chen, J., Li, J., Sun, Y., Wang, Z., Chen, H., Liao, H., Ding, A., Umarji, G.S., Patil, R.S., Chen, Q., Kawamura, K., 2016. Molecular markers of secondary organic aerosol in Mumbai, India. Environ. Sci. Technol. 50, 4659–4667. https://doi.org/10.1021/acs.est.6b00372.

Fu, P., Kawamura, K., Chen, J., Barrie, L.A., 2009. Isoprene, monoterpene, and sesquiterpene oxidation products in the high arctic aerosols during late winter to early summer. Environ. Sci. Technol. 43, 4022–4028. https://doi.org/10.1021/es803669a.

Fu, P., Kawamura, K., Kanaya, Y., Wang, Z., 2010. Contributions of biogenic volatile organic compounds to the formation of secondary organic aerosols over Mt. Tai, Central East China. Atmos. Environ. 44, 4817–4826. https://doi.org/10.1016/j.atmosenv.2010.08.040.

Hong, Z., Zhang, H., Zhang, Y., Xu, L., Liu, T., Xiao, H., Hong, Y., Chen, J., Li, M., Deng, J., Wu, X., Hu, B., Chen, X., 2019. Secondary organic aerosol of PM2.5 in a mountainous forest area in southeastern China: molecular compositions and tracers implication. Sci. Total Environ. 653, 496–503. https://doi.org/10.1016/j.scitotenv.2018.10.370.

Hu, D., Bian, Q., Li, T.W.Y., Lau, A.K.H., Yu, J.Z., 2008. Contributions of isoprene, monoterpenes, β-caryophyllene, and toluene to secondary organic aerosols in Hong Kong during the summer of 2006. J. Geophys. Res. 113 https://doi.org/10.1029/2008jd010437.

Huang, R.-J., Zhang, Y., Bozzetti, C., Ho, K.-F., Cao, J.-J., Han, Y., Daellenbach, K.R., Slowik, J.G., Platt, S.M., Canonaco, F., Zotter, P., Wolf, R., Pieber, S.M., Bruns, E.A., Crippa, M., Ciarelli, G., Piazzalunga, A., Schwikowski, M., Abbaszade, G., Schnelle-Kreis, J., Zimmermann, R., An, Z., Szidat, S., Baltensperger, U., Haddad, I.E., Prévôt, A.S.H., 2014. High secondary aerosol contribution to particulate pollution during haze events in China. Nature 514, 218–222. https://doi.org/10.1038/nature13774.

Jaoui, M., Kleindienst, T.E., Lewandowski, M., Offenberg, J.H., Edney, E.O., 2005. Identification and quantification of aerosol polar oxygenated compounds bearing carboxylic or hydroxyl groups. 2. Organic tracer compounds from monoterpenes. Environ. Sci. Technol. 39, 5661–5673. https://doi.org/10.1021/es048111b.

Jaoui, M., Lewandowski, M., Kleindienst, T.E., Offenberg, J.H., Edney, E.O., 2007. β-caryophyllinic acid: an atmospheric tracer forβ-caryophyllene secondary organic aerosol. Geophys. Res. Lett. 34 https://doi.org/10.1029/2006gl028827.

Kleindienst, T.E., Jaoui, M., Lewandowski, M., Offenberg, J.H., Lewis, C.W., Bhave, P.V., Edney, E.O., 2007. Estimates of the contributions of biogenic and anthropogenic hydrocarbons to secondary organic aerosol at a southeastern US location. Atmos. Environ. 41, 8288–8300. https://doi.org/10.1016/j.atmosenv.2007.06.045.

Kristensen, K., Cui, T., Zhang, H., Gold, A., Glasius, M., Surratt, J.D., 2014. Dimers in α-pinene secondary organic aerosol: effect of hydroxyl radical, ozone, relative humidity and aerosol acidity. Atmos. Chem. Phys. 14, 4201–4218. https://doi.org/10.5194/acp-14-4201-2014.

Lewandowski, M., Jaoui, M., Offenberg, J.H., Kleindienst, T.E., Edney, E.O., Sheesley, R. J., Schauer, J.J., 2008. Primary and secondary contributions to ambient PM in the midwestern United States. Environ. Sci. Technol. 42, 3303–3309. https://doi.org/10.1021/es0720412.

Li, J., Wang, G., Wu, C., Cao, C., Ren, Y., Wang, J., Li, J., Cao, J., Zeng, L., Zhu, T., 2018. Characterization of isoprene-derived secondary organic aerosols at a rural site in North China Plain with implications for anthropogenic pollution effects. Sci. Rep. 8 https://doi.org/10.1038/s41598-017-18983-7, 535-535.

Li, L., Hu, J., Li, J., Gong, K., Wang, X., Ying, Q., Qin, M., Liao, H., Guo, S., Hu, M., Zhang, Y., 2021. Modelling air quality during the EXPLORE-YRD campaign – Part II. Regional source apportionment of ozone and PM2.5. Atmos. Environ. 247, 118063. https://doi.org/10.1016/j.atmosenv.2020.118063.

Li, W., Wang, J., Qi, L., Yu, W., Nie, D., Shi, S., Gu, C., Ge, X., Chen, M., 2020. Molecular characterization of biomass burning tracer compounds in fine particles in Nanjing, China. Atmos. Environ. 240, 117837. https://doi.org/10.1016/j.atmosenv.2020.117837.

Lin, Y.H., Knipping, E.M., Edgerton, E.S., Shaw, S.L., Surratt, J.D., 2013. Investigating the influences of SO2; and NH3; levels on isoprene-derived secondary organic aerosol formation using conditional sampling approaches. Atmos. Chem. Phys. 13, 8457–8470. https://doi.org/10.5194/acp-13-8457-2013.

Liu, J., Shen, J., Cheng, Z., Wang, P., Ying, Q., Zhao, Q., Zhang, Y., Zhao, Y., Fu, Q., 2020. Source apportionment and regional transport of anthropogenic secondary organic aerosol during winter pollution periods in the Yangtze River Delta, China. Sci. Total Environ. 710, 135620. https://doi.org/10.1016/j.scitotenv.2019.135620.

Lyu, X.P., Guo, H., Cheng, H.R., Wang, X.M., Ding, X., Lu, H.X., Yao, D.W., Xu, C., 2017. Observation of SOA tracers at a mountainous site in Hong Kong: chemical characteristics, origins and implication on particle growth. Sci. Total Environ. 605–606, 180–189. https://doi.org/10.1016/j.scitotenv.2017.06.161.

Ming, L., Jin, L., Li, J., Fu, P., Yang, W., Liu, D., Zhang, G., Wang, Z., Li, X., 2017. PM2.5 in the Yangtze River Delta, China: chemical compositions, seasonal variations, and regional pollution events. Environ. Pollut. 223, 200–212. https://doi.org/10.1016/j.envpol.2017.01.013.

Mo, Z., Shao, M., Lu, S., Qu, H., Zhou, M., Sun, J., Gou, B., 2015. Process-specific emission characteristics of volatile organic compounds (VOCs) from petrochemical facilities in the Yangtze River Delta, China. Sci. Total Environ. 533, 422–431. https://doi.org/10.1016/j.scitotenv.2015.06.089.

Nozière, B., Kalberer, M., Claeys, M., Allan, J., D'Anna, B., Decesari, S., Finessi, E., Glasius, M., Grgić, I., Hamilton, J.F., Hoffmann, T., Iinuma, Y., Jaoui, M., Kahnt, A., Kampf, C.J., Kourtchev, I., Maenhaut, W., Marsden, N., Saarikoski, S., Schnelle-Kreis, J., Surratt, J.D., Szidat, S., Szmigielski, R., Wisthaler, A., 2015. The molecular identification of organic compounds in the atmosphere: state of the art and challenges. Chem. Rev. 115, 3919–3983. https://doi.org/10.1021/cr5003485.

Offenberg, J.H., Lewis, C.W., Lewandowski, M., Jaoui, M., Kleindienst, T.E., Edney, E.O., 2007. Contributions of toluene and α-pinene to SOA formed in an irradiated toluene/α-pinene/NOx/air mixture: comparison of results Using14C content and SOA organic tracer methods. Environ. Sci. Technol. 41, 3972–3976. https://doi.org/10.1021/es070089+.

Palm, B.B., Campuzano-Jost, P., Day, D.A., Ortega, A.M., Fry, J.L., Brown, S.S., Zarzana, K.J., Dube, W., Wagner, N.L., Draper, D.C., Kaser, L., Jud, W., Karl, T., Hansel, A., Gutiérrez-Montes, C., Jimenez, J.L., 2017. Secondary organic aerosol formation from in situ OH, O_3, and NO_3 oxidation of ambient forest air in an oxidation flow reactor. Atmos. Chem. Phys. 17, 5331–5354. https://doi.org/10.5194/acp-17-5331-2017.

Paulot, F., Crounse, J.D., Kjaergaard, H.G., Kürten, A., St Clair, J.M., Seinfeld, J.H., Wennberg, P.O., 2009. Unexpected epoxide formation in the gas-phase photooxidation of isoprene. Science 325, 730–733. https://doi.org/10.1126/science.1172910.

Rattanavaraha, W., Chu, K., Budisulistiorini, S.H., Riva, M., Lin, Y.-H., Edgerton, E.S., Baumann, K., Shaw, S.L., Guo, H., King, L., Weber, R.J., Neff, M.E., Stone, E.A., Offenberg, J.H., Zhang, Z., Gold, A., Surratt, J.D., 2017. Assessing the impact of anthropogenic pollution on isoprene-derived secondary organic aerosol formation in PM(2.5) collected from the Birmingham, Alabama, ground site during the 2013 Southern Oxidant and Aerosol Study. Atmos. Chem. Phys. 16, 4897–4914. https://doi.org/10.5194/acp-16-4897-2016.

Ren, Y., Wang, G., Tao, J., Zhang, Z., Wu, C., Wang, J., Li, J., Wei, J., Li, H., Meng, F., 2019. Seasonal characteristics of biogenic secondary organic aerosols at Mt. Wuyi in Southeastern China: influence of anthropogenic pollutants. Environ. Pollut. 252, 493–500. https://doi.org/10.1016/j.envpol.2019.05.077.

Shen, R.Q., Ding, X., He, Q.F., Cong, Z.Y., Yu, Q.Q., Wang, X.M., 2015. Seasonal variation of secondary organic aerosol tracers in Central Tibetan Plateau. Atmos. Chem. Phys. 15, 8781–8793. https://doi.org/10.5194/acp-15-8781-2015.

Shrivastava, M., Cappa, C.D., Fan, J., Goldstein, A.H., Guenther, A.B., Jimenez, J.L., Kuang, C., Laskin, A., Martin, S.T., Ng, N.L., Petaja, T., Pierce, J.R., Rasch, P.J., Roldin, P., Seinfeld, J.H., Shilling, J., Smith, J.N., Thornton, J.A., Volkamer, R., Wang, J., Worsnop, D.R., Zaveri, R.A., Zelenyuk, A., Zhang, Q., 2017. Recent advances in understanding secondary organic aerosol: implications for global climate forcing. Rev. Geophys. 55, 509–559. https://doi.org/10.1002/2016rg000540.

Simoneit, B.R.T., 2002. Biomass burning — a review of organic tracers for smoke from incomplete combustion. Appl. Geochem. 17, 129–162. https://doi.org/10.1016/s0883-2927(01)00061-0.

Stone, E.A., Hedman, C.J., Zhou, J., Mieritz, M., Schauer, J.J., 2010. Insights into the nature of secondary organic aerosol in Mexico City during the MILAGRO experiment 2006. Atmos. Environ. 44, 312–319. https://doi.org/10.1016/j.atmosenv.2009.10.036.

Stone, E.A., Nguyen, T.T., Pradhan, B.B., Man Dangol, P., 2012. Assessment of biogenic secondary organic aerosol in the Himalayas. Environ. Chem. 9, 263. https://doi.org/10.1071/en12002.

Surratt, J.D., Chan, A.W.H., Eddingsaas, N.C., Chan, M., Loza, C.L., Kwan, A.J., Hersey, S. P., Flagan, R.C., Wennberg, P.O., Seinfeld, J.H., 2010. Reactive intermediates revealed in secondary organic aerosol formation from isoprene. Proc. Natl. Acad. Sci. U.S.A. 107, 6640–6645. https://doi.org/10.1073/pnas.0911114107.

Surratt, J.D., Murphy, S.M., Kroll, J.H., Ng, N.L., Hildebrandt, L., Sorooshian, A., Szmigielski, R., Vermeylen, R., Maenhaut, W., Claeys, M., Flagan, R.C., Seinfeld, J. H., 2006. Chemical composition of secondary organic aerosol formed from the photooxidation of isoprene. J. Phys. Chem. 110, 9665–9690. https://doi.org/10.1021/jp061734m.

Szmigielski, R., Surratt, J.D., Gómez-González, Y., Van der Veken, P., Kourtchev, I., Vermeylen, R., Blockhuys, F., Jaoui, M., Kleindienst, T.E., Lewandowski, M., Offenberg, J.H., Edney, E.O., Seinfeld, J.H., Maenhaut, W., Claeys, M., 2007. 3-methyl-1,2,3-butanetricarboxylic acid: an atmospheric tracer for terpene secondary organic aerosol. Geophys. Res. Lett. 34 https://doi.org/10.1029/2007gl031338.

Tang, J.H., Chan, L.Y., Chan, C.Y., Li, Y.S., Chang, C.C., Wang, X.M., Zou, S.C., Barletta, B., Blake, D.R., Wu, D., 2008. Implications of changing urban and rural emissions on non-methane hydrocarbons in the Pearl River Delta region of China. Atmos. Environ. 42, 3780–3794. https://doi.org/10.1016/j.atmosenv.2007.12.069.

Xu, J.-S., Xu, M.-X., Snape, C., He, J., Behera, S.N., Xu, H.-H., Ji, D.-S., Wang, C.-J., Yu, H., Xiao, H., Jiang, Y.-J., Qi, B., Du, R.-G., 2017. Temporal and spatial variation in major ion chemistry and source identification of secondary inorganic aerosols in Northern Zhejiang Province, China. Chemosphere 179, 316–330. https://doi.org/10.1016/j.chemosphere.2017.03.119.

Xu, L., Guo, H., Boyd, C.M., Klein, M., Bougiatioti, A., Cerully, K.M., Hite, J.R., Isaacman-VanWertz, G., Kreisberg, N.M., Knote, C., Olson, K., Koss, A., Goldstein, A.H., Hering, S.V., de Gouw, J., Baumann, K., Lee, S.-H., Nenes, A., Weber, R.J., Ng, N.L., 2015. Effects of anthropogenic emissions on aerosol formation from isoprene and monoterpenes in the southeastern United States. Proc. Natl. Acad. Sci. U.S.A. 112, 37–42. https://doi.org/10.1073/pnas.1417609112.

Yee, L.D., Isaacman-VanWertz, G., Wernis, R.A., Kreisberg, N.M., Glasius, M., Riva, M., Surratt, J.D., de Sá, S.S., Martin, S.T., Alexander, M.L., Palm, B.B., Hu, W., Campuzano-Jost, P., Day, D.A., Jimenez, J.L., Liu, Y., Misztal, P.K., Artaxo, P., Viegas, J., Manzi, A., de Souza, R.A.F., Edgerton, E.S., Baumann, K., Goldstein, A.H., 2020. Natural and anthropogenically influenced isoprene oxidation in southeastern United States and central Amazon. Environ. Sci. Technol. 54, 5980–5991. https://doi.org/10.1021/acs.est.0c00805.

Yuan, Q., Lai, S., Song, J., Ding, X., Zheng, L., Wang, X., Zhao, Y., Zheng, J., Yue, D., Zhong, L., Niu, X., Zhang, Y., 2018. Seasonal cycles of secondary organic aerosol tracers in rural Guangzhou, Southern China: the importance of atmospheric oxidants. Environ. Pollut. 240, 884–893. https://doi.org/10.1016/j.envpol.2018.05.009.

Zhang, H., Surratt, J.D., Lin, Y.H., Bapat, J., Kamens, R.M., 2011. Effect of relative humidity on SOA formation from isoprene/NO photooxidation: enhancement of 2-methylglyceric acid and its corresponding oligoesters under dry conditions. Atmos. Chem. Phys. 11, 6411–6424. https://doi.org/10.5194/acp-11-6411-2011.

Zhang, Q., Streets, D.G., Carmichael, G.R., He, K.B., Huo, H., Kannari, A., Klimont, Z., Park, I.S., Reddy, S., Fu, J.S., Chen, D., Duan, L., Lei, Y., Wang, L.T., Yao, Z.L., 2009. Asian emissions in 2006 for the NASA INTEX-B mission. Atmos. Chem. Phys. 9, 5131–5153. https://doi.org/10.5194/acp-9-5131-2009.

Zhang, Y., Wang, X., Zhang, Z., Lü, S., Shao, M., Lee, F.S.C., Yu, J., 2013. Species profiles and normalized reactivity of volatile organic compounds from gasoline evaporation in China. Atmos. Environ. 79, 110–118. https://doi.org/10.1016/j.atmosenv.2013.06.029.

Zhang, X., Zhao, X., Ji, G., Ying, R., Shan, Y., Lin, Y., 2019. Seasonal variations and source apportionment of water-soluble inorganic ions in $PM_{2.5}$ in Nanjing, a megacity in southeastern China. J. Atmos. Chem. 76 (1), 73–88. https://doi.org/10.1007/s10874-019-09388-z.

Zhu, W., Luo, L., Cheng, Z., Yan, N., Lou, S., Ma, Y., 2018. Characteristics and contributions of biogenic secondary organic aerosol tracers to PM 2.5 in Shanghai, China. Atmos. Pollut. Res. 9, 179–188. https://doi.org/10.1016/j.apr.2017.09.001.